CORROSION Vol 41, no 2 pp 100-104 (1985) February

Corrosion of Bronzes of Shipwrecks

A comparison of Corrosion Rates Deduced from Shipwreck Material and from Electrochemical Methods

R. J. TAYLOR* and I. D. MACLEOD**

Abstract

Data on corrosion of metals are normally derived from two sources, namely, immersion/exposure tests and controlled electrochemical experiments. Because of inherent problems associated with the extrapolation of short-term measurements to long-term performance, many field workers are sceptical of the value of electrochemical data.

In order to compare these two methods, corrosion rate data obtained for bronzes using (1) chemical analysis of corrosion products and (2) instantaneous corrosion rate measurements are presented. The material was examined after 170 years' immersion in tropical waters north-west of Western Australia where the American China Trader "*Rapid*" foundered in 1811. The nature of the corrosion products and the microenvironment will be discussed in terms of pH, oxygen access, E_h gradients, and the microstructure of the objects. Problems associated with non-uniform surfaces and slow rates of attaining a steady state will be discussed. Corrosion rates from the two methods are in good agreement and compare well with literature values for similar materials.

Introduction

Corrosion studies on metals generally fall into two main categories, namely (1) short-term laboratory experiments using electrochemical perturbation techniques and (2) long-term immersion/exposure tests in various controlled environments. Many comparisons of these two approaches have been made for simple systems, but fewer have been made for more complex cases. This paper presents data on the corrosion of bronzes recovered from the wreck of the American China Trader "Rapid," which sank on Monday, January 7,1811, near the North West Cape some 1100 km north of Perth.

On-site measurements of corrosion potentials and pH were conducted after the bronzes' 170 years of exposure in the sea, and, as such, they provide valuable data as long-term exposure tests. Average corrosion currents estimated using the observed depth of corrosion on objects raised from the wreck have been compared with data obtained using instantaneous corrosion rate measurements on the same material in its concreted (i.e., covered with calcareous marine growth) and film-free states. The bronzes have a complex microstructure with various inclusions and casting porosity. The materials used in this work have also been examined by wet chemical, XRD, SEM, optical microscopic, and microprobe techniques.

*Submitted for publication December 1983, revised July 1984

[8]Materials Research Laboratories, Cordite Avenue, Maribyrnong, Victoria, 3032, Australia

** Western Australian Maritime Museum, Fremantle, WA, Australia

Experimental

The wreck of the "*Rapid*" is located approximately 1 km from Point Cloates at 22o44' S, 113 o41' E and is protected from the Indian Ocean swell by a near by coral and limestone reef. The salinity at the site is 35.5 $^{o}/_{oo}$ (i.e., parts per thousand), and the average temperature varies throughout the year within the range of 24.5 ± 3.0 C. The present temperatures are essentially the same as those determined for the period 1811-1812 from measurements of the o18/o16 isotope ratios in the shells of barnacles found on the wreck.[1] The oxygen concentration was determined by Winkler titrations using the standard method and was found to be 80 to 85% saturation (165 to 175µmol/kg) at a depth of 6 m. The oxygen concentration is the sediment varies according to the level, and anaerobic conditions were found at a sediment depth of 0.5m.

Corrosion potentials were measured with a Fluke 8010A-digital multimeter in a waterproof case using platinum to contact the metal surface and a Ag/AgCl (seawater) reference electrode.

The potential of the reference was calibrated on board the support vessel. Surface pH measurements were made using a flat surface Orion electrode (913500) and a portable Pye 293 pH meter. The objects were towel-dried on board the support craft, and pH measurements were made on the surface layers of the corrosion products and on the underlying metal. The surface pH of the copper bars encased in rudder wood was obtained after breaking was obtained after breaking off sections of the wood. All on-site corrosion potential measurements are reported vs SHE, assuming negligible iR drop and that the potential of the Ag/AgCI electrode is the same on the surface as at the depth of 5 to 6 m.

Samples of the metal in the rudder pintles and gudgeons were taken by drilling into sound metal. A section of one of the brace pins was mounted in Araldite (Ciba-Geigy Ltd., Araldite D epoxy resin with hardener HY956 in a ratio of 8:1) and polished to 0.25 μm before SEM and microprobe analysis. Measurements of the depth of corrosion were performed on a set of eight pintles and gudgeons (Figure 1) and rudder bars, the total weight of which was 248 kg with an estimated geometric surface area of approximately 6 m^2.

Instantaneous corrosion rate measurements were performed in aerated synthetic seawater at 22 ± 1 C on specimens derived from the pintle brace pins after a period of storage following recovery from the wrecksite. One sample was machined to a cylindrical shape and attached to a standard electrode holder.[2] The other was machined on both ends of a cylinder, leaving the concreted surface in its as-recovered condition. The bare surfaces were coated with three layers of epoxy resin and attached to an electrode holder as above. The method used for determination of corrosion rates, which has been described previously,[3,4] involves least squares analysis of the polarization curve at potentials less than 50 mV from the corrosion potential. The corrosion current, the polarization resistance, and the anodic and cathodic Tafel parameters were obtained.

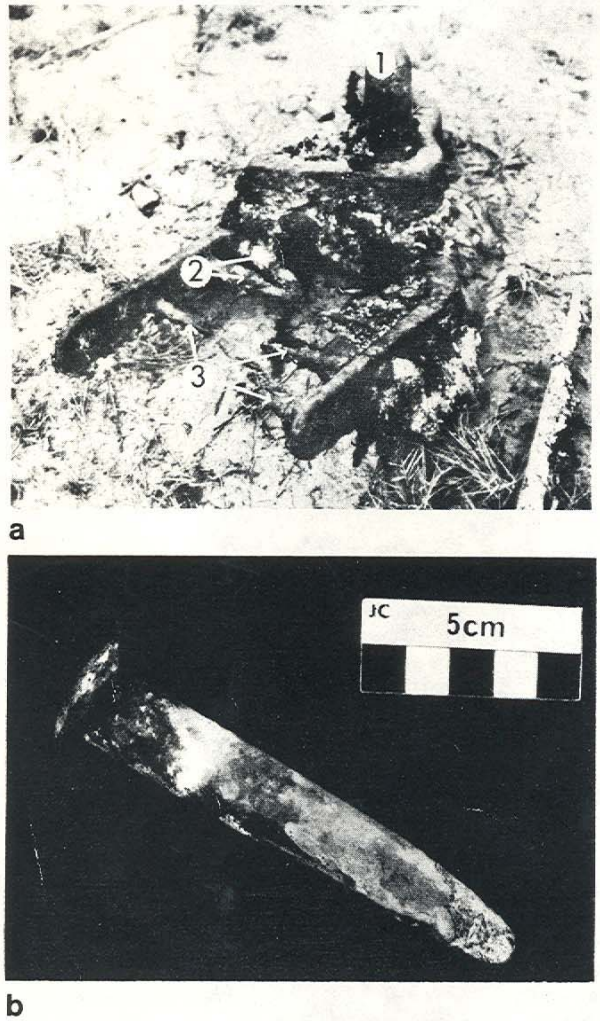

FIGURE 1(a) — Part of the bronze rudder fittings from the wreck of the "Rapid." The pintle (1) still has vestiges of the original rudder wood (2) attached to the brace pins (3). The arms of the gudgeon are broken, and there is some calcareous concretion on the corroded surfaces of the gudgeon (4) and the pintle; (b) detail of brace pin after removal of wood.

Results

Site Measurements

The on-site corrosion potentials of the bronze pintles ranged from +0.040 ± 0.020 V on the seaward corroded surface at pH 8.2, to – 0.004 ± 0.010 V on the freshly exposed metal surface where the p[H varied between 6.2 and 7.6. Inspection of the Pourbaix diagram fro copper in seawater shows that the pintles are in a zone of active corrosion, as shown by Figure 2. The more positive values of the potential on the surface of the rudder fittings indicate a different mechanism and/or rate. The corrosion product layer and any marine concretion form a barrier to the free exchange of oxygen and ionic species.[5,6] The cause of the lower pH of the region adjacent to the metal is due to the hydrolysis of corrosion products, viz.,

$$2Cu^{+} + H_2O \rightarrow Cu_2O + 2H^{+} \quad (1)$$

$$Sn^{2} + H_2O \rightarrow SnO + 2H^{+} \quad (2)$$

Areas of the bronze fittings that had been exposed to oxygenated seawater and were lying on the seabed were

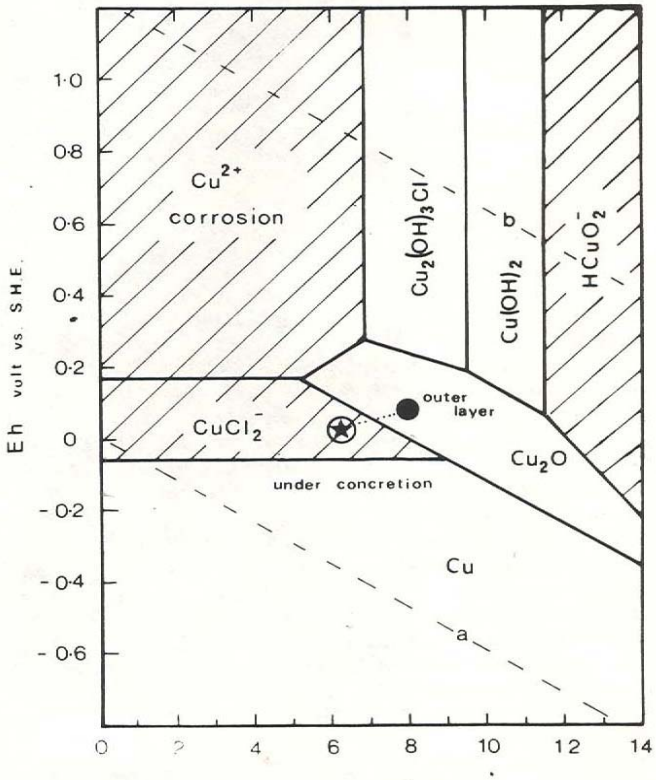

FIGURE 2 — Pourbaix diagram for copper in seawater (Reference 15) showing the surface pH and the *in situ* E_{corr} measurements on the set of bronze pintles and gudgeons from the "Rapid."

TABLE 1 - Composition of Bronzes, Corrosion Products and Associated Fittings from the "Rapid" (1811)

	Cu	Sn	Pb	Zn	Sb	As	Fe
Pintle	91.84	4.78	1.91	0.30	0.12	0.18	<0.02
Pintle brace pin (overall composition)	93 1	5.7	0.68	0.052	0 14	0.15	0.11
Brace pin [(1)] (tin-rich area)	82.4	12.3	0.49	0.74	1.00	0.59	0.07
Corrosion layer on Brace bar	5.15	26.01	5.07	0.75	0.68	0.28	< 0.02
	(13.6) [(2)]	(68.6)	(13.4)	(1.9)	(1.8)	0.70	
Copper bar	99.34	0.12	0.23	0.001	0.06	0.08	<0.02
Rudder wood	36 1	0.32	0.11	0.015	0.022	-	0.23
	(98.0) [(2)]	(0.87)	(0.30)	(0.04)	(0.06)	-	(0.62)

Chemical analysis by atomic absorption spectroscopy (AAS) unless otherwise specified.
[(1)] Electron microprobe analysis
[(2)] Metal analysis normalized to 100%

covered with a thin and adherent layer of blue-green paratacamite [$\gamma Cu_2(OH)_3Cl$] overlying a layer of red-brown cuprite (Cu_2O) and gray-white cassiterite (SnO_2) to a depth of 1.3 mm. Where the bronzes had been partially covered with the loose sand and coral debris, the depth of the corrosion product layer was generally 1.4 to 2.2 mm. Areas of the pintles attached to the rudder wood gave surface pH readings of 5.7 and were corroded to a depth of 3.0 to 3.5 mm. Similar corrosion depths were observed on copper bars that were surrounded by the remains of the rudder wood *(Larix occidentalis*, Western larch).

Microstructure and Corrosion Products

The cast bronze pintles and brace pins were analysed by wet chemical methods and electron microprobe. The results are summarized in Table 1 along with the analysis of the corrosion products found on the pins inside the rudder wood and in the wood itself.

The leaded bronzes have a primary alpha dendritic phase with an alpha plus delta eutectoid as well as non-metallic inclusions. Lead is dispersed as droplets throughout the eutectic phase. By using the low vacuum backscattered electron mode of a modified JEOL SEM, [7] excellent atomic number contrast can be obtained on the polished sections of the brace pins, as seen in Figures 3 and 4, with the lighter areas being tin-rich and the medium gray regions being coper-rich. Cracks in the outer edge of the in are clearly visible in Figure 3. The tin-rich phases have a higher proportion of antimony and arsenic in them than the copper-rich zones (see Table 1), and the selective attack on the tin-rich phase can be seen in Figure 4.

The section of the brace pin nearest the sea suffered massive attack on the alpha phase, but further into the metal, the dendritic eutectoid has been preferentially corroded, as can be seen readily in Figure 4. Deep casting fissures were readily visible to the naked eye in the polished section of the bronze pin. The fittings were manufactured by J. Davis in the Boston area ca. 1807, and so the presence of inclusions and some porosity is not unexpected given that the industry in the United States was in its infancy.

The corrosion products from the pintles and brace pins in the rudder wood were analysed by XRD and wet chemical methods. On the pintle surface, the major corrosion products were cassiterite (SnO_2), cuprite (Cu_2O), paratacamite [γ $Cu_2(OH)_3Cl$] and small amounts of tin oxide sulfate ($Sn_3O_2SO_4$). Such corrosion products are typical for a bronze aerobically corroded in the sea. [8] The tight fit of the rudder wood over the brace pins apparently reduced the ingress of oxygen since the valence of the tin corrosion

FIGURE 3 — A scanning electron micrograph of the seaward surface of a bronze pintle brace pin. The polished transverse section shows copper-rich areas as a medium gray while the tin and lead-rich phases are lighter in tone. The loss of the copper-rich phase close to the seawater interface is readily apparent. Full width is approximately 790 μm.

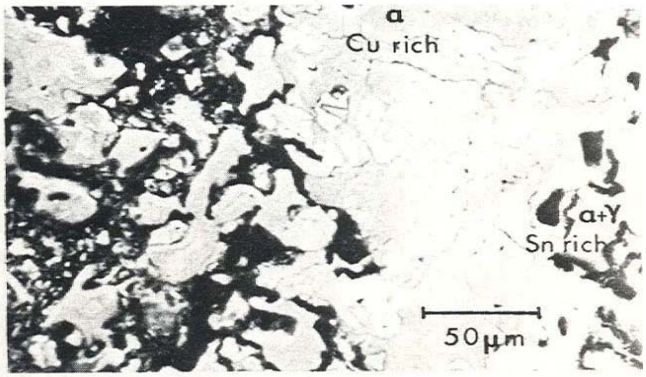

FIGURE 4 — A scanning electron micrograph of a bronze pintle brace pin showing selective removal of the tin-rich (α + γ) phase adjacent to an area of uncorroded metal that shows both the copper-rich and tin-rich phases intact. Full width is approximately 260 μm.

products was more commonly two than four. The major corrosion products were hydromarchite [$Sn_6O_4(OH)_4$], tin oxide (SnO), with smaller amounts of Sn_3O_4 and tin (II) acetate ($SnC_4H_6O_4$). An unusual corrosion product also present in this matrix was the antimony oxide senarmontite, Sb_2O_3. The major copper corrosion product on the pins was cuprite (Cu_2O). The corrosion products in the wood were principally aerobic and consisted of Cu_2O and various forms of basic copper (II) hydroxy chlorides of the general formula $Cu_2(OH)_3Cl$. In areas of wood where anaerobic conditions had developed, the principal corrosion product was chalcocite (Cu_2S).

Electrochemical Measurements

Response to Potential Steps

The method of corrosion rate measurement used involves perturbing the potential of a freely corroding specimen and measuring the current responses. Both the freshly machined and the concreted electrodes had complex current decays showed when potential steps were applied. The current decays showed at least two distinct regions with different time constants. Currents generally reached a steady state after 100 to 1000s, although in some cases, even this period was insufficient and experiments had to be repeated. (The theory for measurement of corrosion rates from polarization curves requires steady-state measurements fro its application.) As a result, the recording of 30-point polarization curves was a time-consuming process lasting up to several hours.

Current decays of the type observed and shown in Figure 5 for these bronze electrodes have been associated with Cole-Cole plots containing multiple semicircles. 12 The transient data were subjected to a Laplace transformation

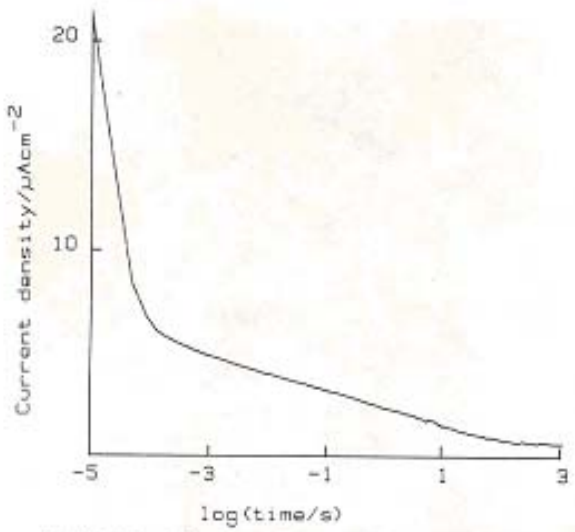

FIGURE 5 — The current-time response to a potential step applied to the concreted bronze pin in synthetic seawater. Each current value is the average from 15 pairs of alternating +5 and −5 mV pulses.

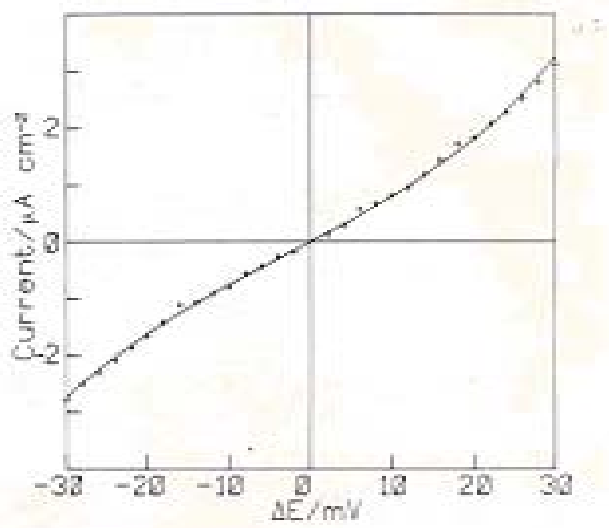

FIGURE 7 — Plot of the current-potential response of the concreted bronze pin in synthetic seawater. The curve is the computed line with the best fit to the experimentally observed data points (+).

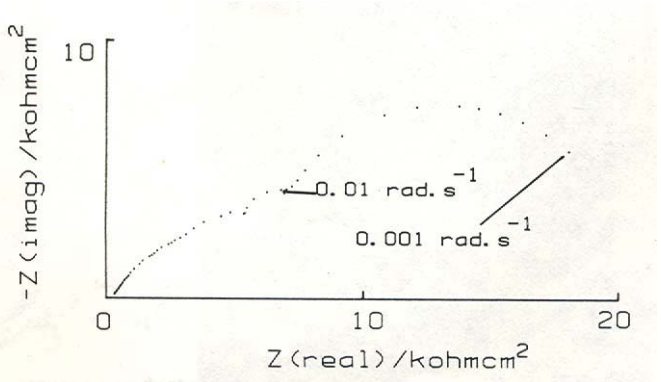

FIGURE 6 — Frequency response diagram for the aged-machined bronze pin in synthetic seawater.

to yield the frequency response for each system. Thus, Figure 6 is an impedance plot for aged machined bronze and clearly shows two semicircles; the concreted bronze had a high frequency response that was more difficult to resolve. It is interesting to note that results similar to these have been observed for single phase 90:10 cupronickel alloys in seawater.[13,14]

Concreted Sample

The potential of the concreted samples became steady at +0.080 ± 0.030 V after 24 hours' immersion; however, solution agitation had no effect on either the corrosion potential or the corrosion current. The corrosion rates, calculated by least squares analysis of the polarization curve (see Figure 7), decreased by an order of magnitude over the first week to a steady value of 0.8 ± 0.2 μA/cm^2 with Tafel slopes b_a = 28 ± 2 mV and b_c = 38 ± 2 mV.

Machined Sample

After four days' immersion in synthetic seawater, the corrosion potential and corrosion current of the bronze pin ceased to be affected by agitation of the solution because an adherent corrosion product had formed on the surface of the sample. The corrosion potential, however, continued to fluctuate slowly with a mean value of + 0.050 ± 0.020 V. The corrosion rates approached a steady value of 1.6 ± 0.3 μA/cm^2 over a seven day period, with Tafel slopes $b_a \cong 46 \pm 2$ mV, $b_c \cong 56 \pm 3$ mV.

Discussion

Since the chemical composition of all the metal objects considered are known (see Table 1) and the densities are documented, it is possible to calculate the number of electrons involved in the overall corrosion process. By assuming that initial oxidation of copper, tin, and lead involves one, two and two electrons, respectively, n, the average number of electrons involved in the oxidation of the objects can be determined and the depth of corrosion converted into average corrosion currents.

The comparison in Table 2 shows good agreement between the values obtained in this study using the electrochemical method and the generally accepted values for bronzes under marine conditions.[9]

The corrosion rate data obtained from measurements based on 170 years of exposure in marine environment are fairly similar to LaQue's data, which are based on a few years' exposure. That the values obtained for concreted and aged machined samples of bronze are virtually identical is not surprising since oxygen diffusion does not appear to be rate controlling under the given experimental conditions, as indicated by the low values for the cathodic Tafel slopes.

The corrosion rates calculated from the long-term exposures must be regarded as minimum values because of the possibility of loss of corrosion product to the marine environment. However, the fact that in many situations the Cu_2O patina preserves the original shape of the object

TABLE 2 - Average Corrosion Currents (μA/cm^2) for Bronzes and Copper in Seawater

	Open Sea	Parity Buried	Adjacent to Wood	N[3]
Bronze fittings "Rapid" (1811)	0.3	0.45	0.8	1.03
Concreted pin	0.8(1) ± 0.2	-	-	1.03
Machined and aged	1.6(1) ± 0.3	-	-	1 03
Copper bars	0.7 to 2 5[2]	-	1.5	1 00
Cast bronze	1 to 2[2]	-	-	-

[1]Data obtained in this work by instantaneous corrosion rate measurements
[2]Data from Reference 9
[3]$_n$ is the average number of electrons involved in the rate-determining process

tends to minimize this source of error when estimating the depth of corrosion. Another explanation of the low value under open seawater conditions is the existence of a differential aeration cell consisting of exposed and concealed sections of the metal objects. Since crevice corrosion of copper base alloys is known,[10] the existence of on-site differential aeration cells is not unexpected. In effect, the concealed sections partially cathodically protect the exposed ones.

Pronounced necking of the copper bars occurred in the areas adjacent to breaks in the encasing wood where the depth of corrosion was approximately twice that of the adjacent areas. Examination of the corrosion patterns and the metallography of the copper bars show that they had been wrought and hot worked. Patches of redeposited copper metal occurred along the length of the bars at the metal/wood interface away from the areas that showed necking. The redeposited metal was free of the trace lead and tin impurities present in the parent bars. The mechanism of this redeposition is not known.

Corrosion Mechanism

The corrosion mechanism of bronze objects on the "Rapid" wrecksite is apparently dependent on the oxygen level of the surrounding water. When bronzes are exposed to well-oxygenated seawater, the copper-rich phase is preferentially attacked, whereas under less oxidizing conditions, the tin-rich (α+*y*), eutectic is selectively corroded. These observations are based on the variation in the nature of the corrosion products on objects of similar composition but of different positioning on the wrecksite profile, and on the metallographic sections of corroded artefacts. Further support for this type of process is found in the work of Campbell and Mills, who studied the corrosion of bell metal in seawater. [11] Analysis of the corrosion products on the surface of the pin that was found with the rudder wood still attached shows a disproportionate amount of tin and antimony (see Table 1). The bulk of the tin corrosion products were divalent, with some mixed Sn^{II}/Sn^{IV} species. The antimony was present as senarmontite (Sb_2O_3) and was probably formed as intermetallic Sn/Sb compounds in the tin-rich phase corroded. Most woods give off acetic acid as their acetate residues are degrade, and some of the wood decomposition products were trapped as tin (II) acetate.

The bulk of the copper corrosion products from the brace pins and pintle arms adjacent to the wood had apparently diffused into the wood, where they were precipitated as either cuprite (Cu_2O) or paratacamite [$yCu_2(OH)_3Cl$] after subsequent hydrolysis and oxidation. The remains of he wood were typically blue-green on the surface with many of the cells filled with cuprite crystals, as shown in Figure 8. Sections of the wood showed areas of elemental copper. Metallic copper probably forms as a result of the $CuCl_2^-$ complex acting as an oxidant in the conversion of organic compounds such as formaldehyde to formic acid. The copper corrosion products apparently protected the timber from attack by wood-boring organisms. Diffusion of the copper (I) chloride complexes along the original longitudinal grain is easier than across the grain; an indication of the relative mobility is found in the shape of the wood that has remained free of attack by wood boring organisms such as the teredo worm. In samples of larch, the ratio of longitudinal to transverse thickness is 5.4 while in American white oak, it was 2.2, the different ratios being largely the result of the fundamental structural differences between a softwood and a hardwood.

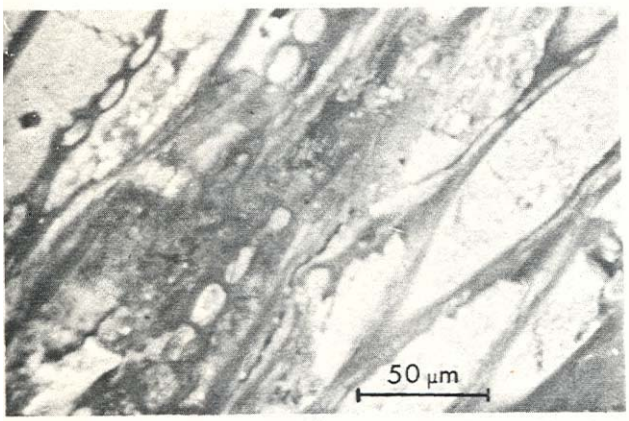

FIGURE 8 — Scanning electron micrograph of a polished section of rudder wood from the "Rapid." Cuprite (Cu_2O) has been precipitated in the vessels of the Larix species as the copper (I) chlorides were hydrolyzed. Full width is 260 μm.

Copper corrosion products are also immobilized by precipitation (hydrolysis and/or oxidation) in the surrounding calcareous concretion that acts as a partial barrier to the free exchange of metal ions and oxygen at the corroding surface.

Conclusion

A comparison of corrosion rates obtained by weight loss data on material recovered from an historic shipwreck and those gained from instantaneous corrosion rate experiments on the same objects show that the latter method provides a good estimate of the corrosion rare that can be expected under the same experimental conditions. Factors such as variation in the amount of dissolved oxygen on the site and the formation of the concretions on the artefacts appear to have a marked effect on the observed corrosion rates.

Acknowledgements

We are in debt to the staff of the CSIRO Division of Mineralogy (Perth) for their assistance with microprobe and SEM measurements. The financial support of the Australian Research Grants Scheme is gratefully acknowledged. We thank Dr. Neil A. North for his help at the shipwreck site and Graeme Henderson for the chance to examine the bronzes.

References

1. I.D. MacLeod, J. S. Killingley, Int. J. Naut. Arch.. Vol. 11. p. 249 (1982).
2. M. Stern, A. C. Makrides, J. Electrochem. Soc., Vol. 107. p. 782 (1969).
3. R. J. Taylor, L. F. G. Williams, Corrosion, Vol. 36, No. 1, p. 41 (1980).
4. L. F. G. Williams, R. J. Taylor, J. Electroanal. Chem.. Vol. 108, p. 305 (1980).
5. N. A. North, Int. J. Naut. Arch., Vol. 5, p. 253 (1976).
6. D. MacLeod, Int. J. Naut. Arch., Vol. 11, p. 267 (1982).
7. B. W. Robinson, E. H. Nickel, Amer. Mineral, Vol. 64, p. 1322 (1979).
8. I. D. MacLeod, N. A. North, Corros. Australasia, Vol. 5. p. 11 (1980).
9. F. F. LaQue, Marine Corrosion - Causes and Prevention. J Wiley and Sons, New York, p. 146, 1976.
10. D. B. Anderson, Galvanic Pitting Corrosion - Field and Laboratory Studies, ASTM STP 576, R. Baboian. W. France. Jr.. L. C. Rowe, J. F. Rynewicz, Eds., ASTM, Philadelphia. Pennsylvania, 1976.
11. H. S. Campbell, D. J. Mills, Metall. Mater. Technol.. Vol. 9. p. 551, 1977.
12. K. Doblhoffer, A. A. Pilla, J. Electroanal. Chem., Vol. 39, p. 91 (1972).
13. L. F. G. Williams. R. J. Taylor, Corrosion, Vol. 38. No. 8. p. 405 (1982).
14. D. D. Macdonald. B. C. Syrett, S. S. Wing, Corrosion. Vol. 34, No. 9, p. 289 (1978).
15. G. Bianchi, P. Longhi, Corros. Sci., Vol. 13, p. 853 (1973).